

Determining the amino acids involved in inhibition of
PDE4B by structurally-diverse compounds

Anni Cai

under the direction of
Dr. Charles S. Hoffman
Boston College

Research Science Institute
July 26, 2011

Abstract

The enzyme phosphodiesterase (PDE) catalyze the degradation of the second messenger cAMP, an important regulator of many cellular transduction pathways, including the production of cortisol and breakdown of lipids. The 11 human PDE families have different tissue distribution and control different pathways. PDE4B, the focus of this study, controls the production of TNF- α in response to bacterial liposaccharide stimulation. Selective inhibition of PDE4B could treat a range of autoimmune diseases. This study identified amino acids involved in PDE4B inhibition and a possible allosteric regulatory site, informing rational drug design of a selective PDE4B inhibitor. We transformed a PDE-deficient strain of *S. pombe* with randomly mutated PDE4B genes generated via PCR. Screening of candidates identified inhibitor-resistant mutant PDEs, which were subsequently sequenced. Comparison of the DNA sequences of these mutant PDE4B with wild-type PDE4B identified amino acid substitutions conferring inhibitor resistance. An aspartic acid to glycine substitution occurred at position 468 in the primary sequence. Structural analysis of the mutant PDE4B reveals a likely allosteric regulatory site close to Gly-468, which is a possible target site for drug inhibitors.

Summary

Phosphodiesterases (PDEs) are enzymes that degrade cAMP, an important molecule in cell signaling pathways. Humans have different types of PDEs which are specific in the pathways they control. PDE4B is involved in inflammatory responses, hence selectively inhibiting it could treat certain autoimmune diseases. This study determined structural characteristics of PDE4B that influences its resistance to chemical inhibitors. We screened for inhibitor-resistant PDEs among randomly generated mutants. Analysis of the mutant structure revealed a possible binding site for a regulatory molecule that could be a target site for inhibitory drugs.

1 Introduction

Phosphodiesterases (PDEs) are a class of related enzymes that degrade adenosine 3'5'-cyclic monophosphate (cAMP) by selectively catalyzing the hydrolysis of the 3' cyclic phosphate bond of cAMP[4].

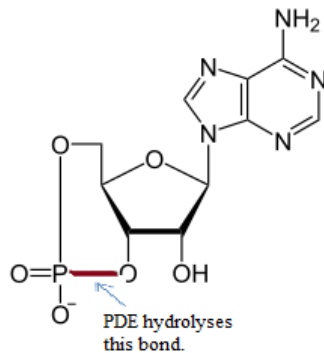


Figure 1: **PDE Action On cAMP.**

PDEs catalyze the hydrolysis of 3' cyclic phosphate bond (shown in bond), thereby converting cAMP to AMP.

PDEs are physiologically important because cAMP is a key second messenger involved in many cellular signal transduction pathways, including production of cortisol and metabolism of lipids. Spontaneous degradation of cAMP by PDEs allows a cAMP-mediated cellular transduction pathway to be quickly terminated once the initial chemical messenger is no longer present, so that the cell may respond to a fresh or repeated signal. This feedback loop forms a basis for the tight regulation of metabolic pathways in response to a fluctuating environment [5].

Human PDEs are categorized into 11 families based on substrate specificity, regulatory properties, and homologies in primary sequence. The various PDEs are encoded by 21 genes, which is transcribed into more than 100 isoforms of the enzyme via alternative splicing. In the official PDE nomenclature, the Arabic numeral specifies the PDE family to which the enzyme belongs, while the capitalized letter represents the gene as reported in Genbank

(NIH genetic sequence database) [4]. Each family has unique substrate selectivity: only the PDE4, PDE7, and PDE8 families act specifically on cAMP; others act on both cGMP (a second messenger similar to cAMP), or on cGMP and cAMP [11].

It has been postulated that some PDEs function solely to prevent “clouds” of cyclic nucleotides from spreading to inappropriate regions of the cell while others regulate local access to specific cAMP/cGMP receptors. Different cell types express unique distributions of PDE isoforms, and the nature and localization of these PDEs are likely to be a major regulator of the local concentration of cAMP/cGMP in the cell [4]. Tissue-specific expression of various PDEs is intimately linked to different physiological functions. For example, PDE1B is implicated in allergic reactions as PDE1B mRNA is responsible for regulating IL-13 in PHA or anti-CD3/CD28-activated human T-lymphocytes. PDE6, predominantly found in rod cells of the photo-receptor layer of the retina, functions in photo-transduction by reducing the steady-state concentration of cGMP in response to light stimulus, thereby leading to the closure of cyclic nucleotide-gated ion channel (CNG) cationic channels. The consequent cell membrane hyper-polarization sends an electric signal through optical nerves to the brain, which is interpreted as a visual stimulus [18].

Much interest has been focused on the PDE4 family in recent years as it was found to influence a number of autoimmune diseases. One of the earliest to be characterized, the PDE4 family was originally named for its selective resistance to rolipram (see Appendix for structure) and is characterized by cAMP substrate selectivity and low K_m values. It comprises 4 isoforms which are sub-categorized into >20 variants that differ in their N-termini, where the PDE4 regulatory domains and phosphorylation sites are located [4]. Studies in knockout mice indicate that each individual PDE4 gene plays a non-redundant regulatory role that cannot be supplanted by the other 3 PDE4 transcripts [12, 20], which agrees with the isoform-specific nature of many PDE-related diseases. One region of the PDE4D gene is linked to heightened risk of ischemic stroke[21], and absence of PDE4D3 led to progres-

sive cardiomyopathy and accelerated heart failure in knockout mice possibly by increasing PKA-mediated phosphorylation of the cardiac ryanodine receptor which rendered the ion channels “leaky” [14]. PDE4B, the focus of this study, regulates inflammatory responses by controlling the the production of TNF- α in both monocytes [12] and macrophages [13] in response to bacterial lipopolysaccharide (LPS) stimulation.

The diversity and specificity of PDEs make them excellent pharmacological targets. Unlike similarly ubiquitous cellular enzymes such as PKA that show no structural variance, each of the structurally different 11 PDE families is involved in different physiological functions. Some pathways are not merely family-specific, but isoform-specific. As such, drugs can be made to target specific disease pathways by selectively inhibiting the specific PDE isoform involved. This can potentially minimize side-effects.

To this end, PDE inhibitor drugs have gained mainstream acceptance. The erectile dysfunction drug, sildenafil (Viagra), is a selective PDE5 inhibitor which prevents cGMP from being degraded, thereby prolonging the signal for smooth muscle relaxation. The consequent vasodilation in the corpus cavernosum optimizes physiological conditions for penile erection [24]. Sildenafil is also used to treat pulmonary arterial hypertension [16] and altitude sickness [19] based on the same mechanism (vasodilation).

Inspired by the pharmacological success of sildenafil, drug companies are increasingly looking towards PDE4 inhibitors as drug candidates. Rolipram, the archetypal PDE4 inhibitor, was originally created by Schering AG as a potential antidepressant and also shows promise for treating inflammatory diseases associated with PDE4B activity, ranging from chronic obstructive pulmonary disease to asthma, arthritis and psoriasis. However, rolipram induces emetic side-effects which are thought to be caused by non-specific inhibition of PDE4D in the brain [15]. Our current research is focused on understanding PDE4B inhibitor-specificity by determining the amino acids involved in inhibition of PDE4B through a novel screening strategy outlined below.

2 Materials and Methods

2.1 Random mutagenesis via PCR

PCR was carried out on plasmid pK63-N21 containing the human PDE4B gene using the FailSafe PCR Kit (Epicentre Biotechnologies, Madison, WI). “Premix” buffers A, B, E, F, K, L (Integrated DNA Technologies, Coralville, IA) containing 100mM Tris-HCl (pH 8.3), 100mM KCl, 400 μ M of each dNTP, varying concentrations of MgCl₂ (3-7mM) and PCR “Enhancer” (0-8X) were used with primers Cgs2-PCRmut-3’ (3’ to open reading frame) 5’AAA GTG TCC GAT GAG AAA AGC GTG 3’ and Cgs2-PCRmut-5’ (5’ to ORF) 5’ TCA TAG CAT ACT TCT TCA CCA AGC 3’. 30 cycles of PCR were performed (each cycle consisted of 30s at 95°C to denature DNA, 30s at 55°C to anneal primers to the template DNA, and 2.5 minutes at 72°C for extension), after which the mutated gene products were collected.

2.2 Screening for inhibitor resistant PDE4B alleles

Schizosaccharomyces pombe strain SP578 (*h⁹⁰leu1-32ade6-17216 cgs2-2*) was transformed following a gap-repair DMSO transformation protocol [2]. Yeast cells were cultured in Yeast Extract Liquid (YEL) medium [9] overnight, then subcultured into Edinburgh Minimal Medium (EMM)(MP Biomedicals, Solon, OH) to target for 10⁷ cells/ml. Cells were then washed with 1X LiOAc/TE buffer ((10 \times LiAc: 1M lithium acetate, adjusted to pH 7.5 with diluted acetic acid; 10 \times TE: 0.1M Tris-HCl, 0.01M EDTA, pH7.5) [2] and brought to a final concentration of 2 \times 10⁹cells/ml in this buffer. Either 200ng (first transformation) or 50ng (second transformation) of StuI-linearized plasmid pKG3-N21 together with an excess of PCR product from each of the 6 PCR reactions and 20 μ g boiled carrier DNA (Sigma Corporation, St. Louis, MO) were mixed with 100 μ l of the prepared yeast cells. The DNA-cell mixtures were incubated for 10 minutes at room temperature, after which 260 μ l of 40% PEG/LiOAc/TE

was added. The mixture was then incubated for 30-60 minutes at 30°C. Following addition of 43 μ l of DMSO solution, the mixture was heat shocked for 5 minutes at 42°C. Following pelleting of cells (centrifugation at 16000 $\times g$ for 5s), removal of supernatant and re-suspension in water, the cell solution was spread onto EMM plates containing 3% glucose, adenine, histidine and uracil, but lacking leucine to select for transformed cells. Plates were incubated at 30°C for five to seven days.

An iodine-staining assay (see Appendix) was performed on colonies to identify candidates that have successfully expressed the human PDE4B gene. Stained colonies were picked and transferred to a 384-well microtiter dish and incubated at 37°C to enrich for vegetative growth relative to mating and meiosis. .

Cells were then transferred to 50 l cultures of EMM-leucine medium in each of 4 plates: 1 control plate containing 0.5% DMSO solution, the other 3 containing compounds 40 M BC27-5, BC35 and BC58 (see Appendix) dissolved in DMSO, respectively. The cultures from each of the compound-containing dishes were screened for ascus formation in the presence of inhibitor compounds, after which the candidates were purified for plasmid rescue.

Purified single colonies were then transferred to liquid YEL-*leu* medium. Cell density was estimated using a cytometer. Cell cultures were diluted to approximately the same order of concentration ($\sim 10^7$ cells/ml). 10 μ l of cell culture was mixed with 10 μ l of DMSO, BC27-5, BC35 and BC58 respectively at 4 μ M concentration in DMSO. 5 μ l of each mixture was plated on agar containing YEL-*leu* medium and incubated at 30°C for 2 days. Colonies were stained with iodine to identify colonies resistant to inhibitors.

2.3 Phenotypic characterization of transformants expressing candidate mutant PDE4B alleles

Selected colonies were transferred to liquid YEL-*leu* medium and incubated at 37°C for 1 day. The cell cultures were then diluted to a concentration of 1×10^7 cells/ml. 10 μ l of cell culture was mixed with 90 μ l of DMSO, and 40 M of compounds BC27-5, BC35 and BC58, respectively to yield 100 μ l of mixture, which is incubated at 30°C for 1 day. Sample solutions from each cell culture were then inspected under the hemocytometer to determine the number of asci, zygotes and stationary phase cells. Mating efficiency was calculated using the formula

$$\text{mating efficiency} = \frac{2(a + z) + \frac{1}{2}s}{2(a + z) + \frac{1}{2}s + p}$$

where a = No. of asci, z = No. of zygotes, s = No. of spores and p = No. of stationary phase cells.

2.4 Plasmid rescue & DNA sequencing

Plasmid rescue from yeast to *E. coli* was done using the Smash and Grab method [10]. The PDE4B2 alleles on the plasmids were PCR-amplified as performed for the initial gap-repair transformations using pre-mix buffer G, purified on a Qiagen spin-column to removed excess PCR primers and sent out to Eurofins MWG Operon (Huntsville, Alabama) for DNA sequencing using custom DNA primers Cgs2-PCRmut-5' (5' TCA TAG CAT ACT TCT TCA CCA AGC 3'), PDE4B2-505F (5'TTC CTC CAT GAT GCG GTC TGT C 3'), and PDE4B2-1165F (5'CAC TGT GCA GAC CTG AGC AAC 3').

2.5 Structural Analysis of PDE4B

PDE4B structure (ID: 2QYL) was downloaded from RCSB PDB (<http://www.pdb.org/pdb/home/home.do>). The protein viewing software Chimera from UCSF (<http://www.cgl.ucsf.edu/chimera/>) was used to analyse the mutant PDE4B enzyme. Residues flanking the pocket was labeled, and the location of hydrophobic and charged residues was determined relative to the pocket to assess its likelihood of being a ligand-binding domain.

3 Results

3.1 Generating PDE4B mutant alleles via PCR

We generated PCR products using 6 different buffers designed to confer different rates and types of mutations. Gel electrophoresis of PCR product samples showed that the gene product was 2.1kb in size, corresponding to that of PDE4B2. All bands were distinct, which shows a large amount of product formed.

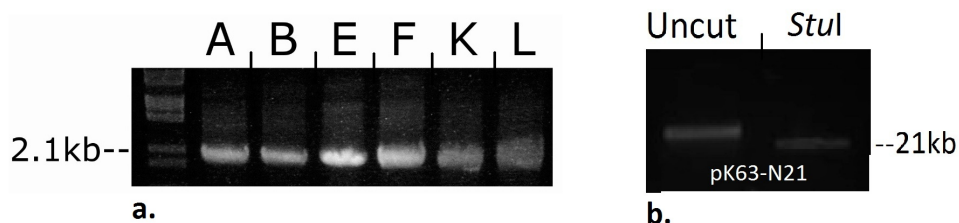


Figure 2: **Gel Electrophoresis Image of PCR Products**

a. PCR products generated using 6 different buffers were all 2.1kb in size, corresponding to that of PDE4B. **b.** The plasmid cut with *StuI* is 21kb in size, and smaller than the uncut circular plasmid.

The band corresponding to the cut plasmid travelled a smaller distance than that of the uncut plasmid, showing successful linearization by *StuI*.

3.2 Transformation of *S. pombe*

Transformation of the first batch of *S. pombe* using 200ng of plasmid vector yielded a lawn of colonies after 48 hours, making the process of picking individual colonies difficult. To decrease colony density, the second batch of cells were transformed using only 50ng of plasmid vector. Number of colonies was reduced 10-fold, resulting in increased colony separation.

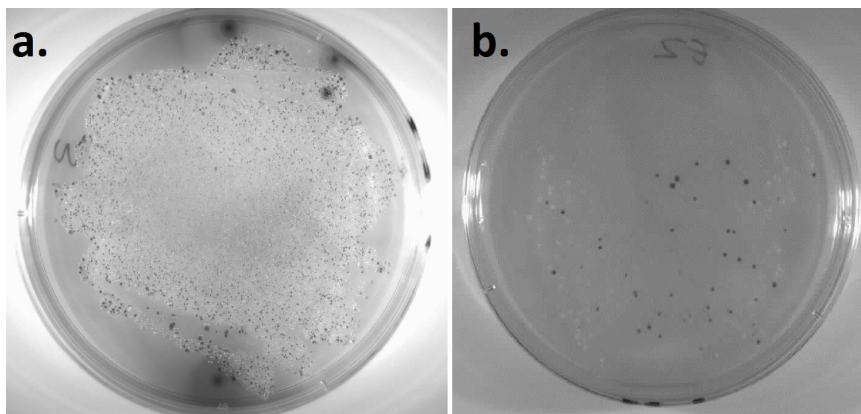


Figure 3: **Comparison of colony density of Batch 1 and Batch 2 transformants**

a. Left plate was transformed using 200ng of plasmid vector, and yielded a dense mesh of small colonies which impeded later efforts to pick individual stained colonies. **b.** Right plate was transformed using 50ng of plasmid vector, and yielded larger colonies with distinct separation.

3.3 Screening for candidate mutants

3.3.1 Iodine Staining

The iodine staining assay identified 318 colonies from the first batch and 257 colonies from the second batch expressing functional (though not necessarily wild-type) PDE genes. However, the first batch yielded dense colonies with poor separation, compromising the accuracy with which stained colonies were picked. The second batch of transformants yielded sparser colonies, allowing colonies to be picked with greater accuracy.

Frequency of stained colonies in each plate vary among the different PCR buffers used for generating the mutant PDE4B allele. Based on visual inspection, the percentage of colonies stained in each plate was estimated. Notwithstanding the limited precision of this type of measurement, it is clear that buffers B and E generated a much higher frequency of stained colonies than buffers K and L.

PCR buffer	Percentage of colonies stained
A	40%
B	60%
E	60%
F	20%
K	5%
L	10%

Table 1: Frequency of stained colonies for different PCR buffers used

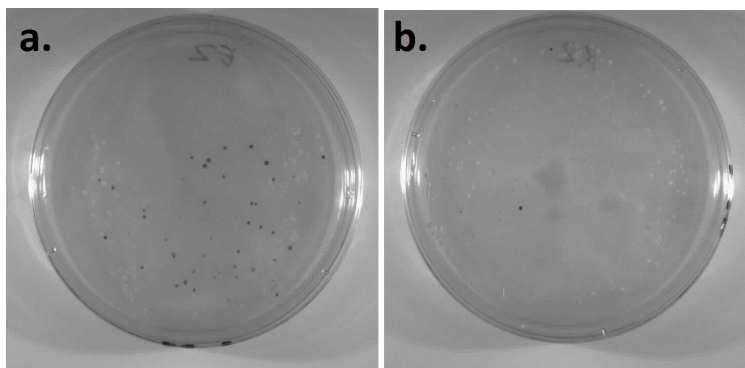


Figure 4: **Different frequency of stained colonies for different PCR buffers**

a. Left plate showed colonies expressing PCR product from buffer E, where more than 60% of colonies were stained. **b.** Right plate showed PCR products from buffer K, where less than 5% of colonies were stained.

3.3.2 Selecting candidates resistant to inhibitor

Mutants of interest have PDEs that function in the presence of inhibitors and can regulate the glucose sensing pathway. Such cells enter into a quiescent state readily in glucose-deficient

medium, presenting with a short, shiny morphology, unlike cells that lack PDE activity and fail to enter stationary phase [7]. There should also be increased mating as reflected by an abundance of zygotes, asci and spores, as cells lacking PDE activity display a severe mating defect [7].

Preliminary screening eliminated colonies showing little mating in the control plate. The remaining candidates were screened for mating or quiescent cells in the inhibitor dishes. Out of 257 preliminary candidates, colonies we named A5, A6, A13, A17, A18, A23, B11, B21, B29, D11, D19, D21, G4, G10, G13, G14, G17, G18 were selected after the second screening.

Following single-cell purification to eliminate contamination of strains, these 18 colonies underwent iodine staining, which identified colonies A18, A23, B21, D19, D21 as clearly inhibitor-resistant.

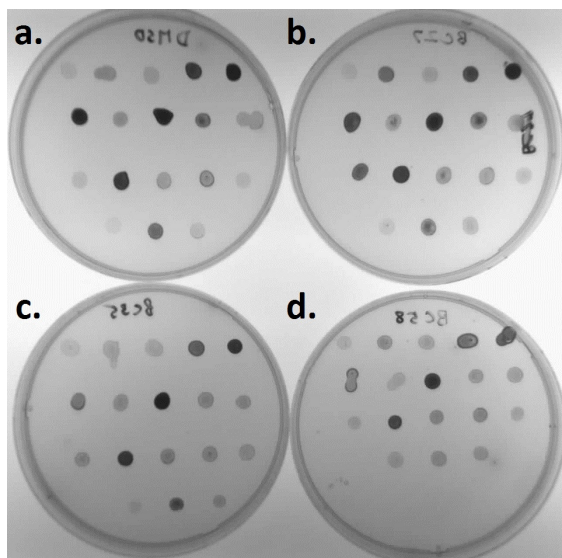


Figure 5: **Result of iodine staining of 18 colonies selected after second screening** DMSO plate generally showed dark staining. In the compound plates, colonies A18, A23, B21, D19, D21 also showed significant staining, suggesting that they express inhibitor-resistant mutant PDE4B alleles.

DMSO plates generally showed darker staining than compound plates. However, D19 showed darker staining in the BC35 plate than in the DMSO plate.

BC58 appears to be the most potent inhibitor in this assay since, the staining was appreciably lighter for most colonies in the BC58 plate as compared to the DMSO plate. Inspection under the microscope also showed that the dish containing BC58 contained the fewest number of asci after an incubation period of 24h.

3.4 Phenotypic characterisation: quantitative mating assay

Results of the quantitative mating assay performed on colonies A18, A23, B21, D19, D21 is shown in Figure 6.

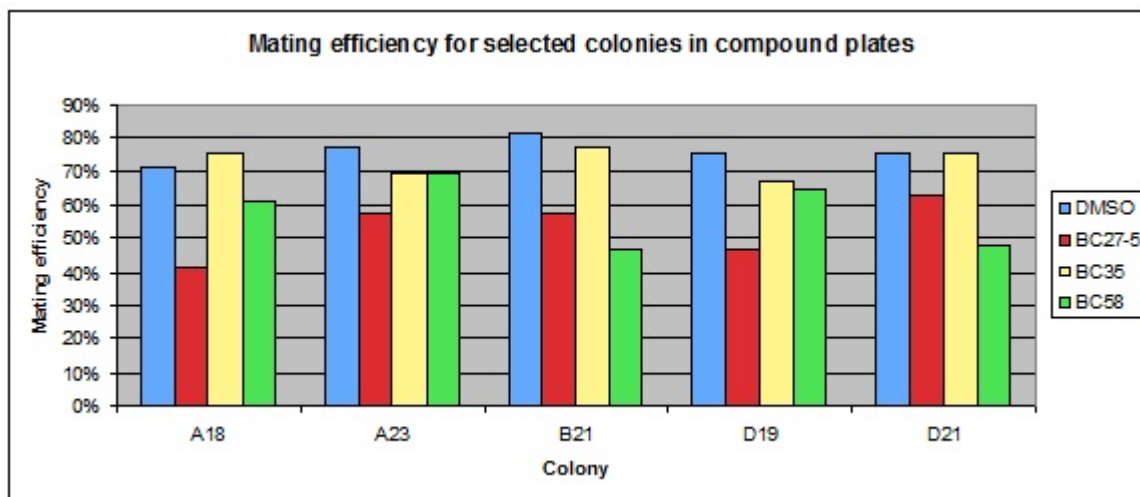


Figure 6: **Results of mating assay**

Colonies in DMSO plates generally showed the highest mating efficiency, consistent with our prediction. A18 was an exception, as it should higher mating efficiency in the BC35 plate than in the DMSO plate.

The results obtained from the mating assay differed from those of the iodine staining assay. Colonies generally showed highest mating in the DMSO plate, with the exception of A18, which showed higher mating in the BC35 plate. BC58 showed most potent inhibition only for 2 of the 5 plates, while BC35 did not show potent inhibition for most plates.

3.5 DNA Sequencing

To investigate the underlying molecular mechanism for inhibition, sequencing was performed on D19. Similar analyses are being performed for the remaining colonies.

Sequencing analysis showed that the mutant PDE4B recovered from colony D19 had an A to G transition mutation at base pair 1403 of the open reading frame, resulting in an aspartic acid to glycine substitution at the position 468 in the primary sequence (NCBI Reference Sequence: NM-001037339.1). Figure 6 shows the location of the amino acid substitution in the 3D conformation of PDE4B, obtained via comparison of the primary sequence with the known crystal structure of PDE4B.

4 Discussion

4.1 Generation of PDE4B mutants & transformation

The different frequency of stained colonies for different buffers may be correlated to the rate and type of mutagenesis that the 6 buffers confer. High rates of mutagenesis may lead to changes in the essential amino acids of the catalytic domain, thus rendering the PDE product non-functional. Future research may be done to confirm whether this result is reproducible to ascertain if the buffer delivers consistent rates of mutation.

4.2 Mating assay

The results of the mating assay differed significantly from those obtained via the iodine staining assay. Random error may be a factor compromising both assays, but each approach has its advantages and drawbacks.

The mating assay here is done under more controlled conditions with the yeast cell concentration fixed across all colonies, as opposed to the solid medium iodine staining assay,

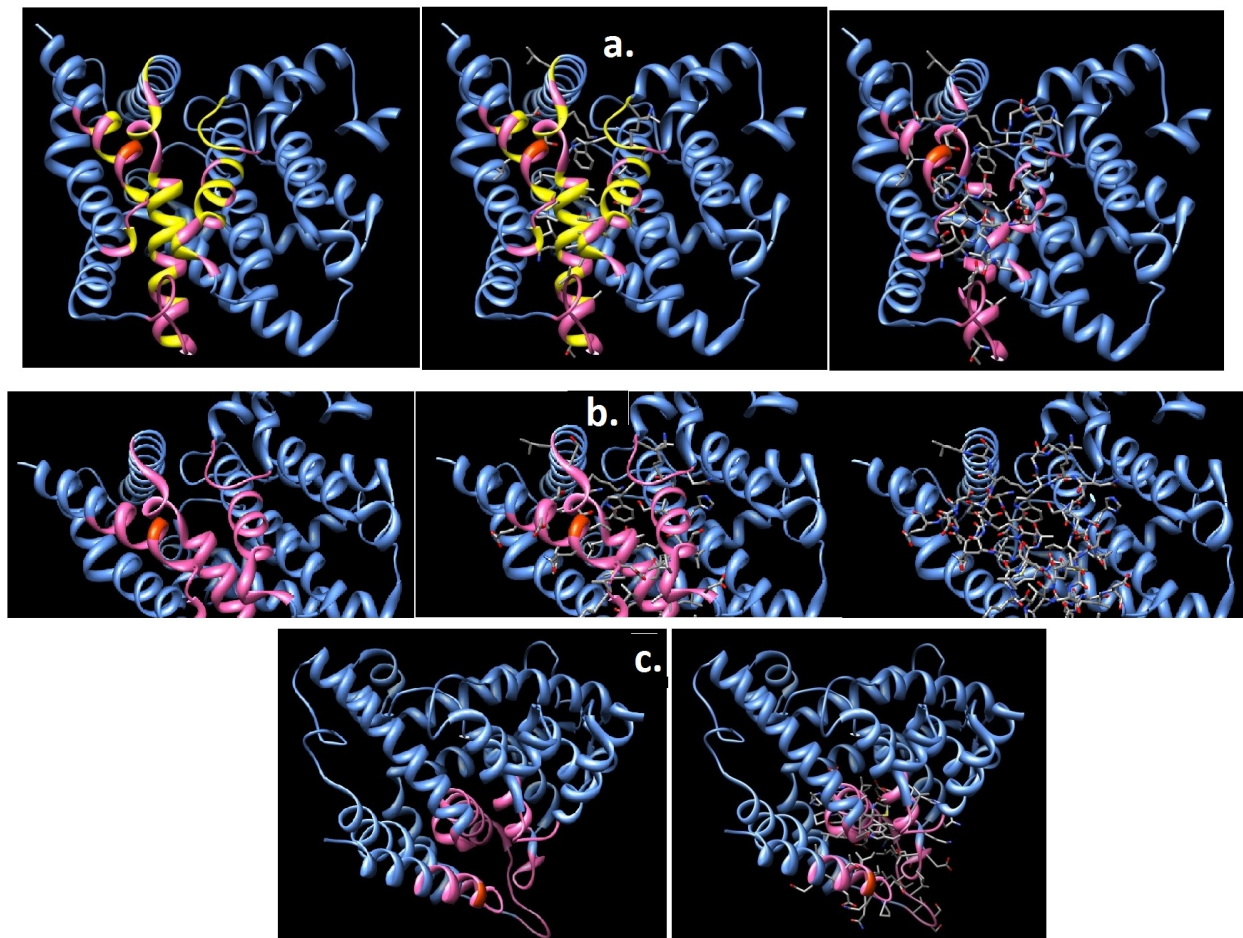


Figure 7: **Model of PDE4B enzymatic structure**

(Pink: Amino acid residues flanking the pocket. Orange: substituted Gly-468. Yellow: hydrophobic residues.) **a.** Pocket is flanked by 3 α -helices and lined with hydrophobic residues, which provides a hydrophobic environment for bound ligands. **b.** A close-up view of the pocket. A disordered loop shields the entrance to the pocket, and may function as a gate. The two fused rings of tryptophan protrudes and blocks entry to the pocket. **c.** Top view of the pocket. Tryptophan is located right in the center, and its bulkiness prevents access by binding ligands.

which concentrations of yeast cells may vary 10-fold. However, the lack of distinct morphological difference between a spore and a stationary phase cell means that counting of cells is liable to human error.

The iodine staining assay is a more robust screening test as high levels of mating must

be present in a colony for it to be stained. Results are representative of the entire colony, unlike the mating assay which is limited by the field of vision of the microscope.

Nevertheless, BC58 appears to be a potent inhibitor in both the mating assay and iodine staining test, having equal or sometimes greater effect than either BC27-5 and BC35. This contrasts with the results of *in vitro* assays [6] which showed that BC58 is 10-fold less potent than BC27-5 and BC35. It is possible that BC58 is more readily uptaken by the cells and thus show greater effect *in vivo*

4.3 Structural Analysis of PDE4B D468G Mutation

Analysis of PDE4B enzymatic structure reveals that the substituted glycine lies at the periphery of a pocket flanked by 3 α - helices and partially covered by a disordered loop. The presence of the disordered loop in between highly ordered α -helices meets the requirements for a gated binding site, separate from the substrate binding/catalytic site. This notion is further supported by the presence of a large tryptophan residue in the center of the pocket, which likely regulates access to the putative allosteric binding site by ligands. The core of the pocket is lined with hydrophobic residues, providing a hydrophobic environment for binding ligands. The periphery of the pocket, however, contains several charged residues that can form electrostatic interactions with charged/polar groups of binding ligands.

The observation that the mutated PDE4B appears to be activated rather than inhibited by BC35 gives rise to interesting possibilities. Firstly, this D468G mutation removes negative charge from the region, altering the electrostatic interactions of that region and possibly affecting binding affinities for charged ligands. This may have caused BC35 to bind in a different orientation, such that it becomes an activator rather than an inhibitor of PDE4B. Furthermore, glycine, by virtue of its small size, breaks the local secondary structure, which may cause drastic conformational changes in the entire pocket.

Much of the uncertainty regarding the precise effect of this D468G mutation arises from

our interpretation of the PDE4B protein crystal structure. protein crystal structures are inherently static, however, and cannot accurately depict enzyme interactions under physiological conditions. Nevertheless, all the evidence discussed above suggest strongly that we have identified a ligand binding pocket in PDE4B that functions as an allosteric regulatory site, and is therefore a possible target for PDE4B inhibitor drugs.

5 Conclusion

This study used a classic chemical genetics approach to determine the amino acids involved in PDE4B inhibition. We generated random mutant alleles of PDE4B, transformed PDE-deficient *S. pombe* hosts with mutated alleles and used the iodine staining assay to screen for inhibitor-resistant candidates. DNA sequencing of PDE4B2 mutant alleles recovered from candidates of interest revealed an amino acid substitution from aspartic acid to glycine near a pocket directly opposite to the active site. Analysis of the mutant PDE4B enzyme revealed strong evidence that the pocket is a ligand-binding domain and functions as an allosteric regulatory site. This information may be useful in rational drug design when creating a PDE4B specific inhibitor.

6 Acknowledgments

I would like to express my profound gratitude to my mentor, Dr. Charles S. Hoffman of Boston College for his invaluable guidance and encouragement throughout the course of this research project. In addition, I would also like to thank Mr. Vinay Tripuraneni for his insightful comments and suggestions for improvement. Last but not least, I would like to thank the Center for Excellence in Education for offering me this opportunity, MIT for hosting this program, and the Ministry of Education, Singapore for its generous funding.

References

- [1] J. Atienza & J. Colicelli. (1998). Yeast model system for study of mammalian phosphodiesterases. *Methods: A Companion to Methods in Enzymology*. 14:35-42.
- [2] J. Bahler, J.Q. Wu, M.S. Longtine, N.G. Shah, A. McKenzie 3rd, A.B. Steever, A. Wach, P. Philippsen, J.R. Pringle. (1998). Heterologous modules for efficient and versatile PCR-based gene targeting in *Schizosaccharomyces pombe*. *Yeast*.14(10):943-51.
- [3] J.A. Beavo, R.S. Hansen, S.A. Harrison, R.L. Hurwitz, T.J. Martins, M.C. Mumby.(1982). Identification and properties of cyclic nucleotide phosphodiesterases. *Mol Cell Endocrinol*. 46:399-405
- [4] A.T. Bender, J.A. Beavo. (2006). Cyclic nucleotide phosphodiesterases: molecular regulation to clinical use. *Pharmacological Reviews* 58:488-520.
- [5] N.A. Campbell, &J.B. Reece. (2008). *Biology 8th edition*. Redwood City, Calif.: Benjamin Cummings.
- [6] D. Demirbas, O. Ceyhan, A.R. Wyman, C.S. Hoffman. (2011). A Fission Yeast-Based Platform for Phosphodiesterase Inhibitor HTSs and Analyses of Phosphodiesterase Activity. *Handbook of experimental pharmacology*. 204:135-49
- [7] J. DeVoti, G. Seydoux, D. Beach, M. McLeod. (1991). Interaction between ran1+ protein kinase and cAMP dependent protein kinase as negative regulators of fission yeast meiosis. *EMBO J*. 10(12):3759-68.
- [8] S.L. Forsburg. (2001). The art and design of genetic screens: yeast. *Nature Reviews: Genetics*. 2:659-668.
- [9] H. Gutz, H. Heslot, U. Leupold and N. Loprieno. (1974). *Schizosaccharomyces pombe*. pp399-446 in *Handbook of Genetics*. 395-446. Edited by R. C. King. Plenum Press, New York.
- [10] C.S. Hoffman & F. Winston. (1987). A ten-minute DNA preparation from yeast efficiently releases autonomous plasmids for transformation of *Escherichia coli*. *Gene*. 57:267-272
- [11] F.D. Ivey, L. Wang, D. Demirbas, C. Allain, & C.S. Hoffman. (2008). Development of a fission yeast-based high-throughput screen to identify chemical regulators of cAMP phosphodiesterases. *Journal of Biomedical Screening*. 13:62-71
- [12] S.L. Jin & M. Conti. (2002). Induction of the cyclic nucleotide phosphodiesterase PDE4B is essential for LPS-activated TNF- α responses. *Proc Natl Acad Sci USA*. 99: 7628-7633.

- [13] S.L. Jin, L. Lan, M. Zoudilova & M. Conti. (2005a). Specific role of phosphodiesterase 4B in lipopolysaccharide-induced signaling in mouse macrophages. *J Immunol.* 175: 1523-1531.
- [14] S.E. Lehnart, X.H. Wehrens, S. Reiken, S. Warriar, A.E. Belevych, R.D. Harvey, W. Richter, S.L. Jin, M. Conti, & A.R. Marks. (2005). Phosphodiesterase 4D deficiency in the ryanodine-receptor complex promotes heart failure and arrhythmias *Cell.* 123:25-35
- [15] B.J. Lipworth. (2005). Phosphodiesterase-4 inhibitors for asthma and chronic obstructive pulmonary disease. *Lancet.* 365: 167-175.
- [16] Pfizer, Inc. (2005). FDA Approves Pfizer's Revatio as Treatment for Pulmonary Arterial Hypertension. 2005 News Releases. Pfizer. Retrieved December 27, 2005.
- [17] R. Pillai, K. Kytle, A. Reyes, & J. Colicelli.(1993). Use of a yeast expression system for the isolation and analysis of drug-resistant mutants of a mammalian phosphodiesterase. *Biochemistry.* 90:11970-11974.
- [18] E.N. Pugh Jr. & T.D. Lamb (2000). Phototransduction in vertebrate rods and cones: molecular mechanism of amplification, recovery and light adaptation. *Molecular Mechanisms in Visual Transduction.* 18:32-55
- [19] J.P. Richalet, P. Gratadour, P. Robach, et al. (2005). Sildenafil inhibits altitude-induced hypoxemia and pulmonary hypertension. *Am. J. Respir. Crit. Care Med.* 171 (3): 275-281.
- [20] W. Richter, S.L. Jin & M. Conti. (2005). Splice variants of the cyclic nucleotide phosphodiesterase PDE4D are differentially expressed and regulated in rat tissue. *Biochem J* 388. (Pt 3): 803-811.
- [21] D. Saleheen, S. Bukhari, S.R. Haider, A. Nazir, S. Khanum, S. Shafqat, M.K. Anis, and P. Frossard.(2005). Association of phosphodiesterase 4D gene with ischemic stroke in a Pakistani population. *Stroke.* 36:2275-2277
- [22] W.J. Thompson, W.L. Terasaki, P.M. Epstein, and S.G. Strada. (1979). Assay of cyclic nucleotide phosphodiesterase and resolution of multiple molecular forms of the enzyme. *Adv Cyclic Nucleotide Res.* 10:69-92
- [23] R.X. Xu, W.J. Rocque, M.H. Lambert, W.D. Holmes, M.A. Luther, W.J. Rocque, M.V. Milburn, Y. Zhao, H. Ke, et al. (2000). Atomic structure of PDE4: insights into phosphodiesterase mechanism and specificity. *Science (Wash DC).* 288:1822-1825
- [24] D.J. Webb, S. Freestone, M.J. Allen, G.J. Muirhead. (1999). Sildenafil citrate and blood-pressure-lowering drugs: results of drug interaction studies with an organic nitrate and a calcium antagonist. *Am. J. Cardiol.* 83 (5A): 21C-28C

A Appendix

A.1 Inhibitor compounds

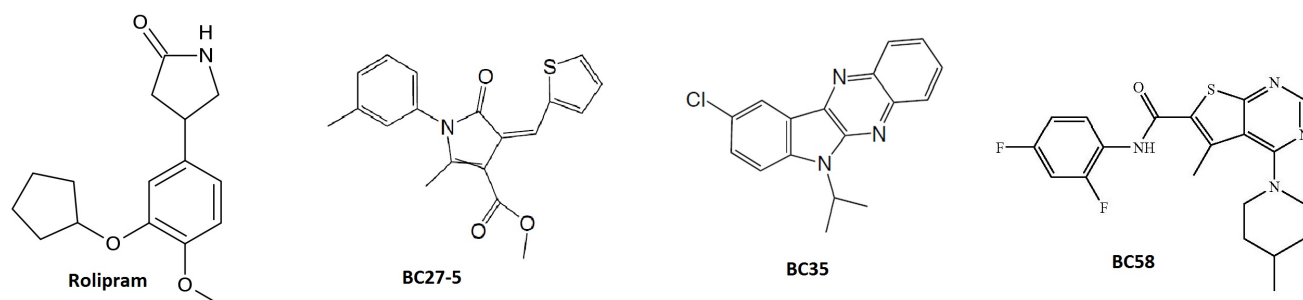


Figure 8: **Known Inhibitors of Rolipram** Rolipram is the archetypal PDE4 inhibitor, for which the family was initially named. BC27-5, BC35 and BC58 were previously identified by the Hoffman lab in an *in vitro* assay as potent PDE4 inhibitors.

A.2 Iodine staining assay

This assay is used to identify colonies expressing a functional PDE. Small iodine crystals are spread on a plate. Each colony plate is inverted and placed on top of the iodine plate, covering the latter. Following 2 minutes of iodine vapor staining, the colony plate is removed. Colonies with high rates of mating are stained.

The basis for this assay lies in a cAMP-mediated glucose sensing pathway that controls mating. In a glucose-deficient environment, no new cAMP is synthesized, so cells with functional PDE will have low cAMP levels, which induces mating. Cells undergoing mating have high levels of glycogen, which stains with iodine. In contrast, dysfunctional PDE cannot degrade cAMP, and cellular cAMP levels is persistently high in the absence of glucose, so no mating occurs.

A.3 Results of mating assay

Colony	Compound	Vegetative cells	Asci	Zygotes	Spores	% mating
A18	DMSO	45	2	49	17	71.06
	BC27-5	61	2	15	18	41.35
	BC35	18	1	14	50	75.34
	BC58	18	0	11	12	60.87
A23	DMSO	13	1	17	17	77.39
	BC27-5	16	7	2	7	57.33
	BC35	12	2	5	27	69.62
	BC58	12	0	11	10	69.23
B21	DMSO	7	3	9	14	81.58
	BC27-5	16	0	8	12	57.89
	BC35	15	1	20	19	77.44
	BC58	18	0	3	20	47.06
D19	DMSO	17	4	19	12	75.36
	BC27-5	19	1	6	6	47.22
	BC35	14	3	5	25	67.06
	BC58	14	2	6	19	64.56
D21	DMSO	15	1	16	23	75.21
	BC27-5	18	2	10	13	62.89
	BC35	12	2	6	43	75.76
	BC58	24	0	8	12	47.83

Table 2: Mating efficiencies of colonies in different compound plates

A.4 PDE4B enzymatic structure

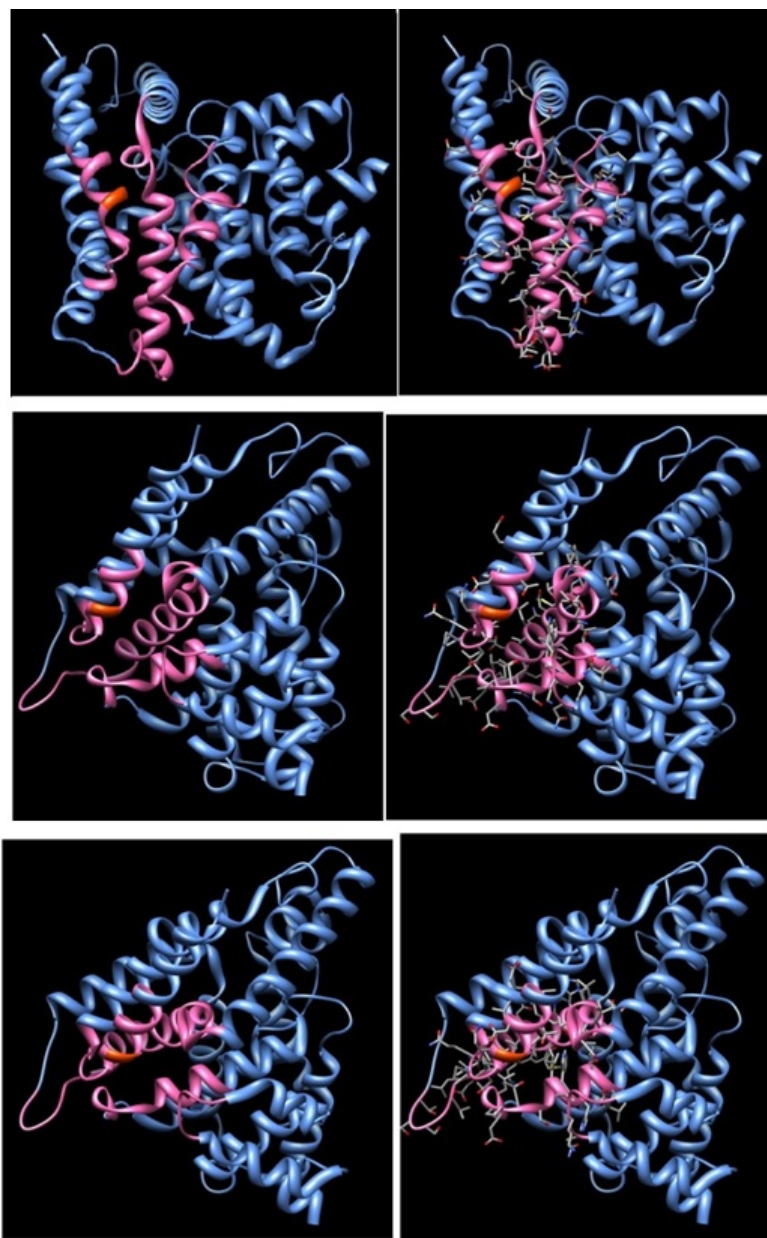


Figure 9: **Additional PDE4B enzymatic structures**

Different views of the PDE4B enzyme. Pink: Residues flanking the pocket are colored pink. Orange: Substituted Gly-468. Different panels show the ribbon structure (left), ribbon structure (right).

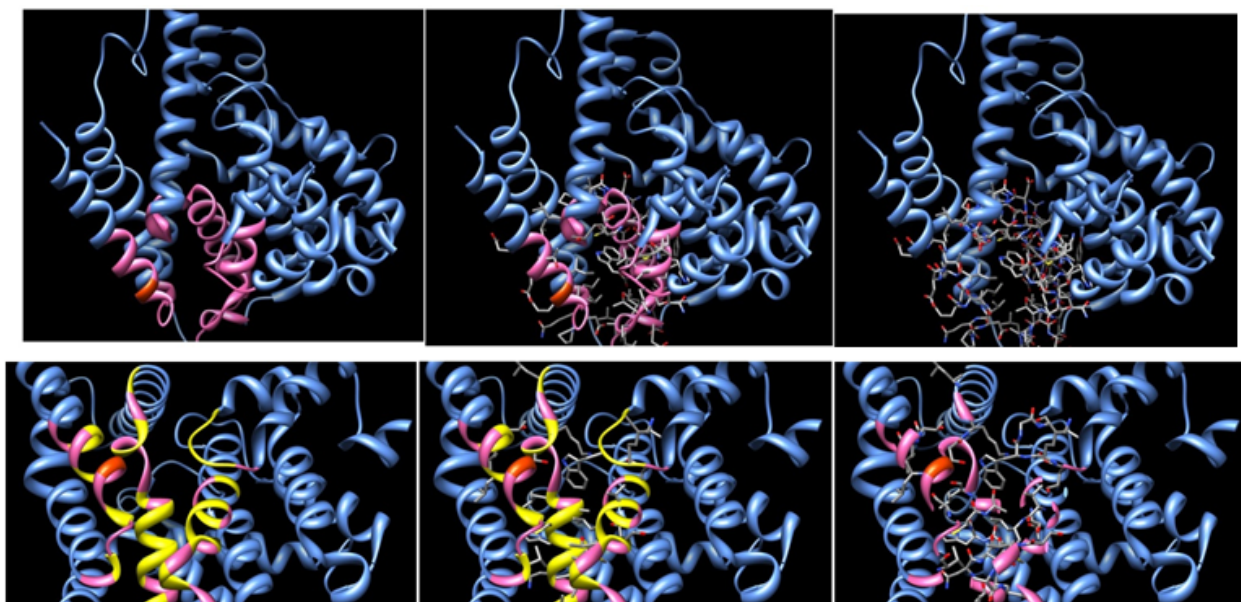


Figure 10: **Additional PDE4B enzymatic structures**

Yellow: Hydrophobic residues Different panels show the ribbon structure (left), ribbon structure and stick structure (center) and stick structure only (right).